FACTA UNIVERSITATIS
Series: **Electronics and Energetics** Vol. 38, Nº 1, March 2025, pp. 127 - 149
https://doi.org/10.2298/FUEE2501127G

Original scientific paper

UNCERTAINTY OF THE RENEWABLE ENERGY ACCESSING THE DISTRIBUTION SYSTEM FOR OPTIMAL VOLTAGE ENHANCEMENT AND MINIMIZATION OF LOSSES USING GORILLA TROOP OPTIMIZATION

Shubash Kumar Guriro[1], Muhammad Suhail Shaikh[2*], Chandar Kumar[3], Shahid A. Iqbal[4]

[1]Dr. G. M Panhwar Institute of Knowledge Learning and Skills, Sindh Pakistan
[2] School of Physics and Electronic Engineering, Hanshan Normal University, Guangdong, China
[3]Department of Electrical Engineering DHA, Suffa University, Karachi, Sindh, Pakistan
[4]Department of Electrical Engineering, SVKM's Institute of Technology, Dhule, India

ORCID iDs:	Shubash Kumar Guriro	https://orcid.org/0000-0002-7087-0242
	Muhammad Suhail Shaikh	https://orcid.org/0000-0003-1082-8664
	Chandar Kumar	https://orcid.org/0000-0002-7354-5955
	Shahid A. Iqbal	https://orcid.org/0000-0003-2815-8304

Abstract. *In recent decades, wind turbines (WT) and solar panels (PV) have been integrated into electrical power systems, particularly within power distribution networks. Given the rising energy demands and the variability of renewable energy sources, the design, operation, and control of power networks have become increasingly challenging. This research focuses on the reduction of technical losses and the enhancement of voltage levels within distribution systems by harnessing the capabilities of solid-state transformers (SST) to provide dual-reactive power support. It assesses the impact of load demands and the integration of distributed generation (DG) units, such as PV and WT, while incorporating SST into the distribution system. The study employs the K-medoid algorithm in a data-driven approach to analyze load demand, solar irradiance, and wind speed. Six test cases are formulated to evaluate the synergistic effects of combining SST with DG technologies, including wind turbines, PV arrays, and batteries. A gorilla troop optimization (GTO) algorithm is employed to determine the optimal placement and sizing of SST, WT, PV, and BES to optimize voltage levels and minimize energy losses in radial power distribution networks. To validate the results, all six cases are compared against IEEE 33 bus data from radial distribution systems, demonstrating the superior performance of the GTO approach in all cases. This study achieved a significant improvement in the voltage profile compared to the current configuration. Active power losses were cut by 82.36% thanks to the optimization of SSTs with dual reactive power support and variable DG, as*

Received July 27, 2024; revised August 13, 2024; accepted August 19, 2024
Corresponding author: Muhammad Suhail Shaikh
Hanshan Normal University, Guangdong, China.
E-mail: suhail.shaikh@live.com

opposed to the existing distribution system. Reactive power losses were also reduced by 86.36%, and the voltage profile saw a marked enhancement, rising from 0.92 p.u. to 1.0 p.u., demonstrating a substantial improvement. Reactive power usage decreased by 71.19%. The study presents a novel solution for long-standing problems related to high distribution system losses and low voltage levels by integrating SSTs with DG systems.

Key words: *Distributed Generations, Power Loss Reduction, Voltage Improvement, Gorilla Troop Optimization*

1. INTRODUCTION

1.1. Background and Related Work

Today's electrical grid makes use of renewable energy sources (RES). For a greener tomorrow, renewable energy sources like solar panels and wind turbines should be prioritized in the electrical grid. With rising demand and penetration levels and the intermittent nature of renewable energy resources, power system planning, operation, and control are becoming increasingly challenging [1-2]. Voltage fluctuations at the consumer's terminal, a rise in load demand, and a deterioration in system efficiency can all be traced back to power losses in the distribution network and its auxiliary equipment, such as the bus and line [3-5]. To improve the dependability and stability of contemporary power systems [6], minimizing the effects of power quality metrics such as voltage dips, harmonics, and power losses is important. Reactive power impacts power quality because it mitigates grid voltage fluctuations, boosts power transfer, and lessens line losses when handled adequately by control devices [7-8]. For proper appliance operation, users require a remarkably stable supply voltage [9]. To keep the voltage acceptable within the limit, the reactive power assistance (RPA) must support reactive power demand and sustain bus voltages [10]. Distribution systems use capacitor banks to improve the power quality in the voltage/power profile issue and lower the cost of power losses. By strategically placing capacitor banks, we can cut down on the bus and the current, reducing reactive power. The uncertainty characteristics of renewable DGs also need to be factored into the optimal deployment of energy storage systems (ESS) and capacitor banks for the optimization process to be carried out and for the findings to be valid in the microgrid uncertainty associated with photovoltaic (PV) and suitable probability functions must adequately characterize wind turbine (WT). Reactive power compensators adjust voltage profile, power losses, greatest voltage rise, and voltage fluctuations, on-load tap changing transformers, and voltage regulators used by distribution and utilization companies and their workers. [11-12]. Control strategies and additional devices are used to increase the quality of power of a distribution system integrated with renewable energy sources [13]. Flexibility in AC transmission systems (FACTS) devices is critical in improving several aspects of the power quality in highly renewable penetration systems [14-17]. When it comes to dealing with the harmonics concerns that arise in a renewable energy system, voltage stabilization, and loss improvement, various FACTS devices have been proposed. These include the thyristor-controlled series capacitor, static var compensator, and static synchronous compensator (STATCOM), and the unified power quality controller (UPQC) is used for voltage profile improvement and harmonics mitigation in grid-connected hybrid renewable energy sources [18-19].

Advanced control methods for converters establish a vital link between the utility grid, aiding in the provision of reactive power, which serves to minimize power losses and voltage fluctuations [20-21]. This research delves into the operation of battery energy storage systems within distribution networks, enabling them to supply reactive power ancillary (RPA) through voltage source converters. The effectiveness of these devices in loss prevention hinges on their specific location and size, a point that remains consistent across all cases discussed in the existing literature. As a result, contemporary power networks demand flexible and adaptable planning strategies to accommodate the variable influx of renewable energy resources (RES). Recent research papers related to optimization [22] have put forth a spectrum of approaches for controlling microgrids and integrating renewable energy resources. In [23], the study contrasts Backpropagation Control (PCA) and Synchronous Reference Frame Theory (SRFT) in terms of power factor control within a radial distribution system. [24] introduces a hybrid optimization technique involving shuffling frog jumping and particle swarm optimization to enhance voltage profiles and reduce losses in radial distribution systems. [25] presents the Binary Particle Swarm Optimization and Shuffled Frog Leap (BPSO-SLFA) algorithms for the optimal placement of distributed generation in radial distribution systems, aiming to improve voltage profiles and minimize power losses [26] suggests the strategic placement of capacitors and PV systems for the reduction of power losses in radial distribution systems. Furthermore, [27] employs a hybrid optimization approach for capacitor relocation and reconfiguration, thus enhancing the overall performance of the distribution system. The utilization of Firefly Optimization [28] in a radial distribution system aids in determining the optimal placement and sizing of capacitors. [29] employs the Modified Whale Optimization (MWO) technique for estimating the parameters of both three-phase and single-phase transmission lines. In [30], Grey Wolf Optimization is employed to optimize parameters for three-phase transmission lines. In [31] explores a hybrid approach involving the HHOPSO algorithm for voltage-constrained reactive power planning, which demonstrates a substantial reduction in active power losses and operational costs, while preserving voltage stability.

To reduce transmission losses through the strategic use of capacitors, [32] recommends employing the Oppositional Crow Search Optimization technique. In [33] introduces a flux linkage method for predicting transmission line parameters in systems with bundled conductors. This method utilizes power-flow equations to enhance the accuracy of transmission-line parameter estimation, particularly in terms of temperature correction resistance, thus improving the overall efficiency of power system operation. Recently, there has been an uptick in interest in a distribution transformer powered by power electronics, specifically, the solid-state transformer. It is a lighter, more functional replacement for the fundamental frequency transformer. It is smaller, has fault tolerance, energy routing, and reactive power support, and is meant to replace the existing transformer [34]. A good illustration of this would be the employment of devices and circuits made from solid-state semiconductor material, which make it possible to control current and voltage profiles. Furthermore, the voltage source converters could be capable of handling a controlled DC bus., which may link to the microgrid [35-36]. It is hypothesized that it might be used as a volt/var control device, in which it would either inject or absorb reactive electricity to/from the grid in order of total voltages. In [37] and [38], research has been done on the possibility of utilizing SST to supply auxiliary grid services. The authors of [39] constructed an SST model to analyze the effect of changing a standard metal transformer. In [40], Radial distribution losses in solid-state transformers can be minimized owing to dual reactive power correction. The authors of this research suggested employing particle swarm optimization to locate and scale SST installations to reduce network losses.

1.2. Motivation and Incitement

With the advent of technological progress, the demand for electrical energy has surged, presenting challenges in both its generation and distribution. Over the past few decades, renewable energy resources (RES), including wind turbines and photovoltaic systems, have been incorporated into power distribution grids. Coping with the growing energy demand and the intermittent nature of renewable sources has made it increasingly complex to plan, operate, and manage power systems. Different studies in the literature have revealed that weak distribution networks and line losses at low voltage levels result in the wastage of electrical power. These issues have led to investigations into reactive power compensation techniques employing power electronic compensators, capacitor banks, and various other methods. More recently, there has been a substantial focus on modifying Solid-State Transformers (SSTs) to provide additional support to distribution systems. This research is aimed at improving the voltage levels within a radial distribution system while simultaneously reducing power losses, taking advantage of the reactive power compensation capabilities of SSTs. Additionally, this study seeks to perform a technical evaluation of a distribution system that integrates distributed generation sources such as photovoltaic systems, wind turbines, and battery energy storage (BES). The analysis accounts for variations in daily load, solar irradiation, and wind speed on an hourly basis.

In addressing these challenges, the most up-to-date strategies using Gorilla Troop Optimization have been applied to find the optimal solution, offering a multi-faceted approach to the problem.

- The proposed approach is novel because it uses optimization to integrate SST, DG, and BES in planning distribution networks.
- Capabilities for more rapid convergence
- Lower calculation times, resulting in more straightforward computations
- Using the same settings for several problems
- Easy to implement

1.3. Contribution and Organization

The main contribution of this proposed work is as follows.

- This research uses the dual reactive power compensation feature of a solid-state transformer in a radial distribution system considering the variability of load demand, energy storage system, and renewable energy generation from wind turbine and photovoltaic systems.
- Gorilla troop optimization (GTO) is used to optimize the placement and number of photovoltaic (PV), wind turbine (WT), and battery energy storage (BES) while accounting for solar irradiation and wind speed variation along with Solid state transformer (SST) and it is compared with GA [41] and PSO [42].
- This analysis considers hourly data on annual load demand, solar irradiance, and wind speed over a year.
- The yearly datasets are partitioned into 24 groups representing the 24 hours of the day by using the K medoid algorithm. This clustering method comes close to recreating the randomness of data samples collected daily during a year.
- This research aims to determine and optimize the voltage of a radial distribution system by comparing the voltage at the system's least-voltage-disturbed nodes to a common value.
- Another goal of this research is to minimize the power losses within the radial distribution network.

However, there are a few limitations of the proposed model with SST integration such as the cost of SST is comparatively high as the cost of conventional transformers and the limited reduction

In the following section 2, the system simulation of a radial distribution system is presented: Section 3 provides load flow analysis showing the effects of PV, WT, and SST: Section 4 provides the proposed parameter and its setting for the simulation of case studies: Section 5 provides the research methodology and short overview of Gorilla troop optimization as well as K-medoid algorithm for the data-driven process. Section 6 shows the proposed method's result and discussion, and the article is finally concluded in section 7.

2. PROPOSED SYSTEM SIMULATION

Electric power is distributed to consumers through a network that encounters a myriad of factors impacting its stability, including consumer diversity, load fluctuations, weather variations, pricing structures, and other variables. Consequently, the distribution system exhibits inherent volatility, unreliability, and inherent unpredictability as mentioned in Fig. 1. To obtain more precise results, it is essential to formulate an optimization model that accommodates fluctuations in load demands. Moreover, when the network incorporates distributed generation (DG) devices such as wind turbines or photovoltaic panels, the system model must account for the intermittent output from these DG units. In the context of clustering, items are organized into classes or clusters based on their similarity to other objects within their cluster and dissimilarity from those in other clusters. Clustering serves as a valuable technique for uncovering meaningful relationships within a dataset. Clustering methods prove instrumental in detecting and interpreting patterns within extensive datasets, including parameters like wind speed, solar irradiance, and load requirements. The K-medoid algorithm is deployed for these clustering techniques, encompassing data sources like solar resource information and annual wind speed statistics, extracted from [43], and annual load demand data derived from [44]. This approach closely emulates the inherent unpredictability of daily data samples collected from a broader dataset spanning an entire year.

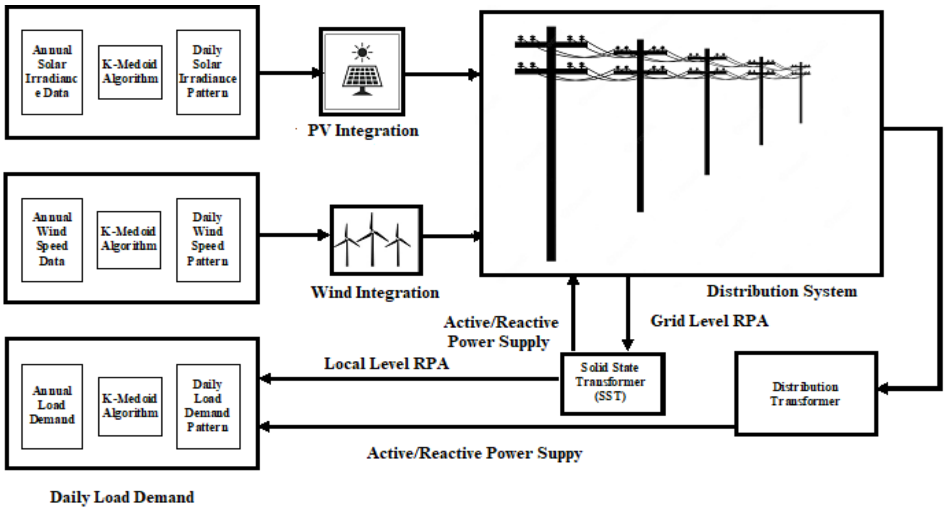

Fig. 1 Representation of the proposed system

2.1. Wind Speed Simulation

This research uses K medoid clustering to partition a yearly wind speed database into 24 hourly clusters. Wind speed patterns are the same year-round as on a single day. Each cluster should occur daily at any moment. Each group has a unique wind speed range.

Fig. 2(a) illustrates the multistep wind speed curve derived by transforming the 24 clusters returned by the K medoid method. In addition, the power output of each wind speed cluster is calculated by applying Eq. (1) shown in Fig. 2(b) to the wind power curve shown there. This allows for a more accurate assessment.

$$P_{WT} = \begin{cases} 0, & v < v_{in} \\ P_{WTR} = \left(\dfrac{v - v_{in}}{v_r - v_{in}}\right), & v_{in} < v < v_{rated} \\ P_{WTR}, & v_r < v < v_{out} \\ 0, & v \geq v_{out} \end{cases} \tag{1}$$

Winds below the cut-in speed, v_{in} generate no power, whereas winds over this threshold do. After going faster than v_r, the output power must still be held to P_{WTR}. To prevent rotor damage, wind turbines are stalled at a speed more significant than the shutdown speed, which is denoted by the constant v_{out}. To bring the rotor to a halt, a braking mechanism is employed.

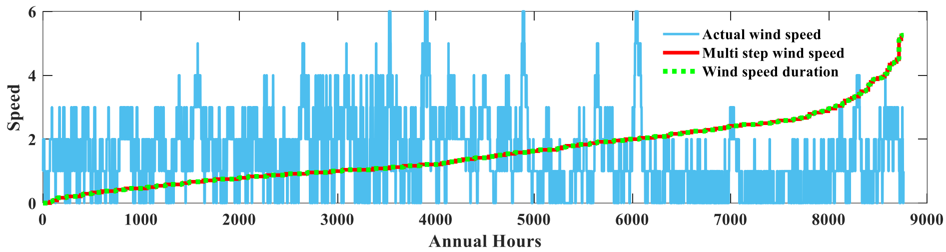

(a)

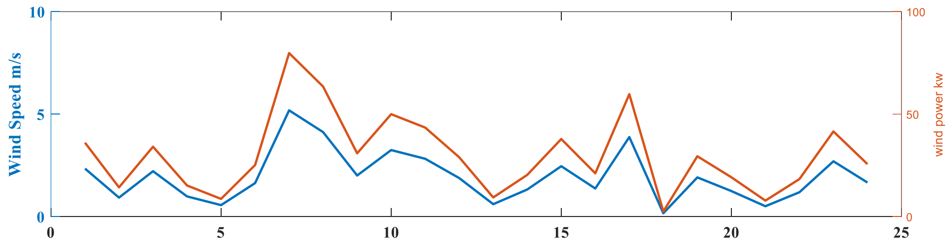

(b)

Fig. 2 (a) Wind speed curve (b)Wind speed and active power output

2.2. Solar Irradiance Simulation

In this study, K-medoid clustering divides an annual sun irradiance database into 24 hourly clusters. The performance patterns of photovoltaic cells are consistent throughout the year, just as they are on any given day. Every cluster ought to take place daily at any time. Irradiance levels might differ significantly between groups due to their different compositions. As observed in Fig. 3, K-medoid clusters are converted into multistep solar irradiance curves. The P_{PV} power output can be determined once the solar irradiation S_{IE} has been evaluated using the following relations.

$$S_{IE} = \frac{I_{SC}.S_{STC}}{I_{SCSTC}[1+K_{mpt}.(T_{module}-T_{amb})]} \tag{2}$$

$$P_{PV} = P_{STC}\cdot\frac{S_{IE}}{S_{STC}}.[1+K_{mpt}.(T_{module}-T_{amb})] \tag{3}$$

where
P_{PV}, Maximum Power of PV module
P_{STC}, Power at standard test conditions, (1000Wm^{-2})
S_{IE}, Effective solar irradiance
S_{STC}, Solar Irradiance at standard test conditions
K_{mpt}, Maximum power temperature coefficient
T_{module}, PV module temperature
T_{amb}, Ambient temperature
I_{SC}, Short circuit current of photovoltaic module
I_{SCSTC}, Short circuit current at standard test conditions

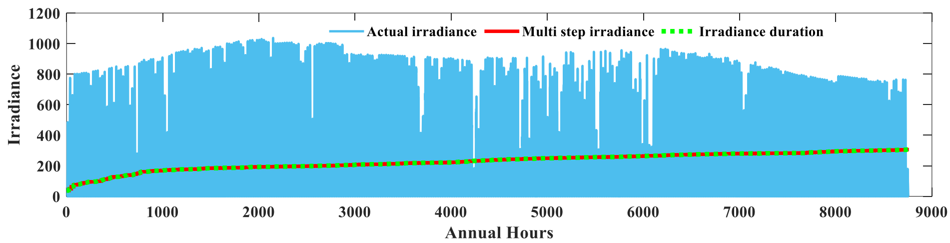

Fig. 3 Multistep solar irradiance curve

2.3. Load Demand Modeling

A database of yearly load demands is partitioned into 24 clusters using the K medoid clustering method. To get the per-unit demand profile, we divide the annual demand profile by 95% of the most outstanding value in the annual data. Specifically, this is done so that the per unit data only exceeds the peak load level of 1.0 p.u. This indicates that a load of 1.0 p.u. is assured when the cluster analysis has been performed. Fig. 4 (a) illustrates the multistep load duration curve and it is assumed that the load pattern will be the same as that observed on a single day, as shown in Fig. 4 (b).

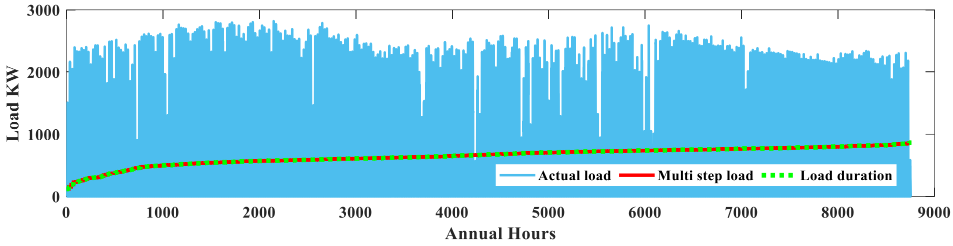

(a)

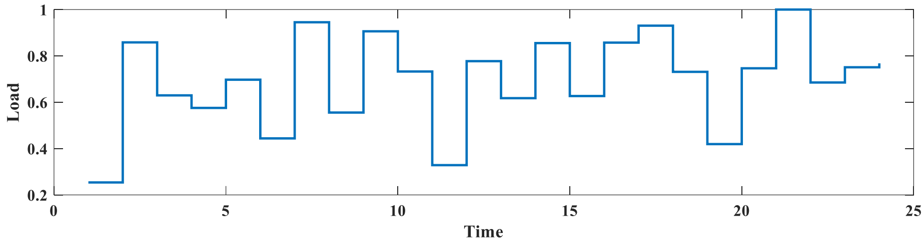

(b)

Fig. 4 (a) Load duration curve (b) Daily load deviation curve

The load demand imposed on a bus q at any particular time can be calculated using the following equations,

$$P_{D,q}(t) = v_f(t).P_q \tag{4}$$

$$Q_{D,q}(t) = v_f(t).Q_q \tag{5}$$

P_q, Q_q is the load demand on bus q, $v_f(t)$ is the variation factor on a time basis. This work's real and reactive power loads fluctuate according to the same factor. Thus, it is assumed that the power factor is consistent in the baseline scenario.

2.4. Reactive power compensation modeling for Solid-State Transformer (SST)

The SST is a power electronics-based transformer with many benefits, including higher efficiency, reduced size, increased fault tolerance, and the ability to provide reactive power. These benefits have led some to argue that the SST is a viable alternative to the traditional transformer. Fig. 5 shows the standard SST design, and Table 1 provides a summary of the roles played by each step.

In this study, the reactive power support capabilities of Stage I inverters and Stage III inverters were utilized. While stage I provides grid-reactive power Q_{SSTG} to manage load bus voltage, stage III is capable of supporting load reactive power demand Q_{SSTD} locally. Estimating the grid reactive power support level requires using the growth rate in the stage-I converter's apparent power rating. If the actual power requirement of the load at the bus q for the t^{th} hour of the day is λ % more than the stage-I converter rating, then it is possible to express $S_{RR,q}(t)$ as in Eq. (6), the reactive grid power can be represented in Eq. (7).

Stage 1:

$$S_{RR,q}(t) = (1+0.01..\lambda)..P_{D,q}(t) \tag{6}$$

where,
S_{RR}, Rate of Rising of Apparent power rating.
P_D, Real power demand

$$Q_{SSTG,q}(t) = \sqrt{(S_{RR,q}(t))^2 - (P_{D,q}(t))^2} \tag{7}$$

Stage 2:

Stage II only supports the load real power and can be rated lesser than stage –III.

Stage 3:

As an additional note, the reactive power source rather than the network is used to provide the load, as shown in Eq. (8).

$$Q_{SSTG,q}(t) = Q_{D,q}(t) \tag{8}$$

SST's dual-reactive power capacity uses stages I and III for reactive power.

In cases where the SST's rating is higher than the load rating, the situation is presumed that it can bear the entire weight; otherwise, the SST and DT will share the load. Let's say a load bus is rated S_{LB} KVA. SST's perceived power capacity is proportional to load rating, thus:

$$S_{SST} = \lambda.S_{LB} \tag{9}$$

Where,
S_{LB}, Definite load bus
λ, SST rating of the load rating

Stage-III inverters supply real power to the load bus at an angle that corresponds to a power factor, φ, and the SST represents the local reactive power demand, expressed by Eq. (10) and Eq. (11), respectively.

$$P_{SST} = S_{SST}.\mathrm{Cos}\,\phi \tag{10}$$

$$Q_{SST} = \gamma.S_{LB}.\mathrm{Sin}\,\phi \tag{11}$$

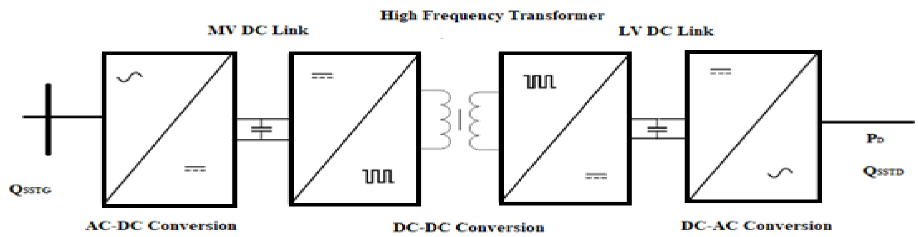

Fig. 5 Schematic arrangement of Solid State Transformer [35]

Table 1 Summary of the roles played by each step of SST [1]

Stage	Purpose	Input	Output
Stage-I	AC-DC Conversion	MV AC	HV DC
Stage-II	DC-DC Conversion	HV DC	LV DC
Stage-III	Supply to Load	LV DC	LV AC

2.5. Loss Modeling of Solid State Transformer and Distribution Transformer

The losses of n^{th} transformer ($P^n_{L,DT}$) can be calculated as in given Eq. (12), [45].

$$P^n_{L,DT} = P^n_{NLL,DT} + P^n_{SCL,DT} \cdot \left(\frac{P_{D,q}}{S^n \operatorname{Cos}\phi} \right)^2 .ALF \tag{12}$$

SSTs could replace old distribution transformers by offering grid flexibility and control, such as power routing or RPA, according to distribution system research. Recent research shows SST is less effective than a conventional transformer. Power converters add hard-to-estimate conductivity and switching losses. SSTs are expensive, with three times the loss of regular distribution Transformers [46]. This article uses an SST approximation loss model, as shown below.

$$P^n_{L,SST} = \alpha_{SST}.S_{SST} \tag{13}$$

Where,
$P^n_{L,DT}$, Actual losses of distribution transformer
$P^n_{NLL,DT}$, No load losses of distribution transformer
$P^n_{SCL,DT}$, Short circuit losses of distribution transformer
S^n, Rated capacity of nth distribution transformer units
Cos φ, Power factor
ALF, Annual load factor
$P^n_{L,SST}$, Losses of SST
α_{SST}, The capacity factor of SST configuration
S_{SST}, Rated capacity of SST.

3. Load Flow Analysis

The forward-swept direct power flow analysis method is used in this article. Power support for both the active and reactive bus comes from the negative loads. Analyzing the DT and SST losses, an additional load is placed on the system in the form of losses. For a bus q, the kVA demand at the t^{th} hour is computed as,

$$S_{D,q}(t) = \left(\sqrt{(P_{D,q})^2} \right) \times (t) + \left(\sqrt{(Q_{D,q})^2} \right) \times (t)\, ; q = 1 | N_{bus} \tag{14}$$

The corresponding equivalent current injection for bus q at i^{th} iteration is computed as,

$$I^i_q(t) = I^r_q(V^i_q) + j(I^i_q)(V^i_q) \tag{15}$$

where,
$S_{D,q}$ is apparent power demand at q^{th} bus
$P_{D,q}$ is active power demand at q^{th} bus
$Q_{D,q}$ is reactive power demand at q^{th} bus
V_q^i is bus voltage at ith iteration for q^{th} bus
I_q^i is Equivalent current injection at ith iteration for q^{th} bus
I_q^r and I_q^i is accurate and imaginary parts of equivalent current injection at the i^{th} iteration for q^{th} bus

The actual power demand of the buses with wind and photovoltaic DG's can be calculated as:

$$P_{D,q}(\delta_{WT}^m) = P_{D,q}(\delta_{WT}^m) - P_{WT}(\delta_{WT}^m) + P_{DT}(\delta_{WT}^m) \tag{16}$$

$$P_{D,q}(\delta_{PV}^m) = P_{D,q}(\delta_{PV}^m) - P_{PV}(\delta_{PV}^m) + P_{DT}(\delta_{PV}^m) \tag{17}$$

where wind and photovoltaic DG position is represented by δ_{WT}^m, δ_{PV}^m respectively and m varies until wind turbine and photovoltaic units m_{WT} and m_{PV}.

The actual power requirement for *SST* buses is computed as,

$$P_{D,q}(\delta_{SST}^m) = P_{D,q}(\delta_{SST}^m) + P_{SST}(\delta_{SST}^m) \tag{18}$$

SST position is represented by δ_{SST}^m m varies till the number of SST units m_{SST}.

The real power requirements of a Distribution transformer (DT) are,

$$P_{D,q}(\delta_{DT}^m) = P_{D,q}(\delta_{DT}^m) + P_{DT}(\delta_{DT}^m) \tag{19}$$

where δ_{DT}^m represents load bus m varies till the number of DT units m_{DT}.

Now, the reactive power requirement can be calculated as:

$$Q_{D,q}(\delta_{SST}^m) = Q_{D,q}(\delta_{SST}^m) - Q_{SSTL,q} - Q_{SSTG,q} \tag{20}$$

The branch current is obtained from the following backward sweep method.

$$I_{br}^i(t) = BIBC \times I_q^i(t) \tag{21}$$

BIBC is the direct load flow bus injection to the branch current matrix [47]. The forward sweep method updates the voltage on each load bus.

$$V_q^i(b_{r_{RE}})(t) = V_q^i(b_{r_{SE}})(t) - I_{br}^i(t) \times Z_{br}; b_r = 1|N_{br} \tag{22}$$

where, $b_{r_{RE}}$, $b_{r_{SE}}$, N_{br} and Z_{br} represents the receiving end bus, sending end bus, number of branches, and branch impedance, respectively. After performing the necessary modifications to the voltage, the voltage errors can be verified at each bus to verify voltage convergence. BIBC simplifies nodes beyond branch detection, saving computation time.

3.1. Problem Formulation and Objective Function

$$f_1 = (\Delta V_{S,\min})^2 q = 1 \big| N_{bus} \quad (23)$$

$$f_2 = (I_{br}^2 \times R_{br}(t))_{br} = 1 \big| N_{br} \quad (24)$$

$$\min(f_{1,} f_2) \quad (25)$$

4. Proposed Parameter Setting

The IEEE 33 bus radial distribution network serves as the test system for this particular piece of research. A bus system with the IEEE 33 standard operates at 12.66 kV and 100 MVA and has an apparent power demand of 436.35 kVA. Table 2 contains the results of several simulation settings in their respective values.

To determine the operating constraints of SST during stage III, the following Eq. (26) is utilized.

$$S_{III}^q(t) = S_{D,q}(t) S_{D,q}(t) \le S_{SST}^{ICR} \quad (26)$$

where, $S_{D,q}$ is the total load demand at the q^{th} bus for the t^{th} hour of the day, and S_{SST}^{ICR} is the individual SST capacity rating.

Table 2 Parameter Setting

Parameter	Values
K_{mpt}	2
T_{module}	20 ºC
P_{STC}	20 W/m^2
S_{STC}	12 W/m^2
P_{WT}	300 kW
v_{in}	4.5 m/s
v_r	13 m/s
v_{out}	25 m/s
V	1.0 p.u
γ	37.3 W/kVA
S_{SST}	500 kVA

5. Proposed Methodology

The main objective of this research is to analyze the performance of the radial distribution system integrated with distributed generation considering a solid state transformer, which includes transformer and SST losses, as well as their effect on the power losses and voltage profile of the distribution system. The suggested GTO algorithm is shown in Fig. 6.

5.1. K-Medoid Algorithm

Unsupervised machine learning algorithm K-medoid clusters data. It partitions to select k exemplary samples [48]. A finite dataset's medoid is the data point with the lowest average dissimilarity. Initialize k cluster medoids by randomly selecting k components from the set.

1. Distances between S elements and medoids are calculated. Each data point has a medoid.
2. Update Medoids to update the editor while incurring as little loss as possible, and we must replace the old Medoid with all the other (m-1) points in the cluster. The following cost function determines minimum loss.

$$M_1, M_2, ...M_k = \arg\min \sum_{i=1}^{k} \sum_{xin} \| x - M_i \Pi^2 \tag{27}$$

3. Repeat: Then repeat steps 2 and 3.

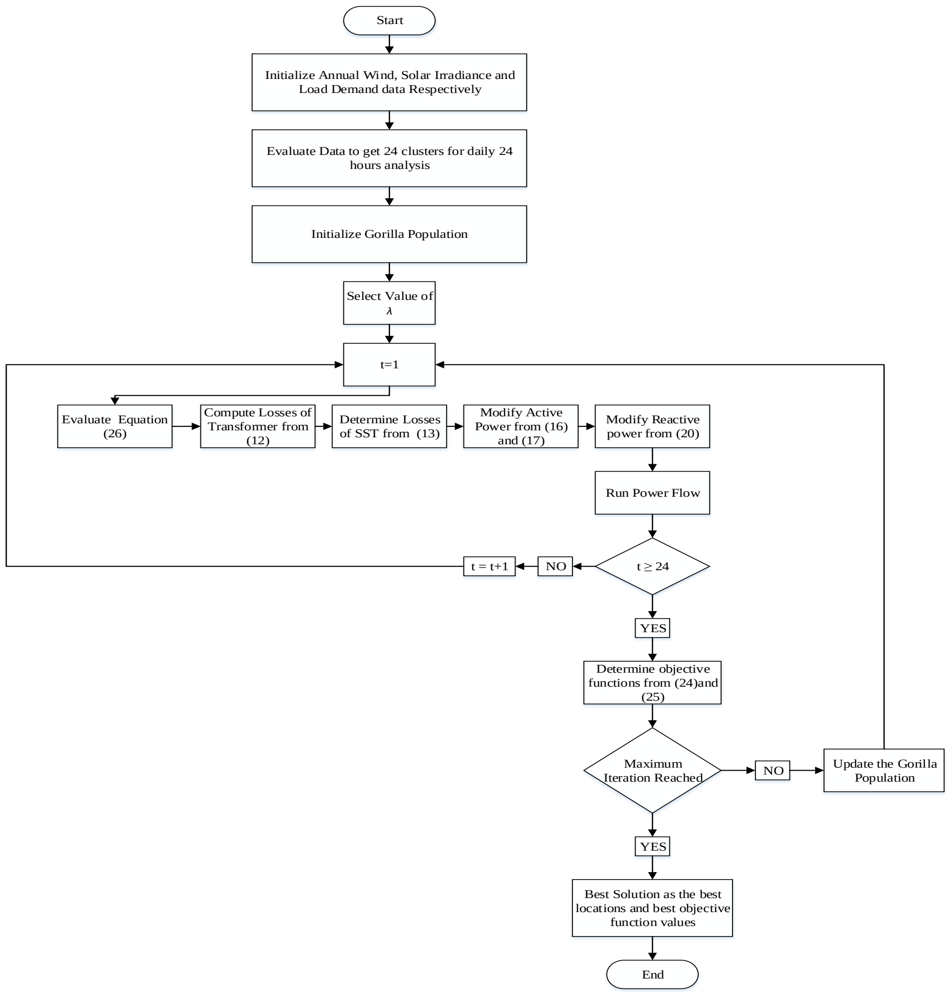

Fig. 6 Proposed GTO Flowchart

5.2. Gorilla Troop Optimization Technique

Optimization is the mathematical process of determining the most efficient, cost-effective, or highest-performing solution to a problem by adjusting certain variables within given constraints [49]. Gorilla troop optimization is a new metaheuristic algorithm based on the social behaviors of groups of gorillas. The two phases of the algorithm, exploration, and exploitation, are fully explained in the paper using mathematical principles [50]. The GTO method simulates optimization tasks (exploration and exploitation) by using five different operators, all named after different things gorillas do. During the exploration phase, three different operators have been used to move to an uncharted area to improve GTO exploration. With the second operator, the gorillas' main goal changes from exploring to taking advantage of what they find. By adding migration toward a known destination as the third operator in the exploration phase, the GTO is much better able to search for different optimization spaces. But in the exploitations phase, we use two operators, which improve search performance.

5.2.1. Exploration Phase

At each GTO stage, the best candidate solution is a silverback gorilla. Exploration strategies include Movement to other gorillas to increase GTO exploration balance exploitation and exploration and migrate towards a known site to increase GTO's search capability. When rand is less than a specific value (p), the migration technique to an unknown location is selected. In addition, a migration strategy toward other gorillas has been selected if the rand is less than 0.5, and a migration in the direction of an already designated place is selected if the rand is more significant than 0.5. The following is a mathematical formulation of the three tactics used during the exploration phase.

$$GX(t+1) = \begin{cases} (UL-LL)\times r_1 + LL rand < p \\ (r_2 - C) + X_r(t) + L \times H, rand < 0.5 \\ X(i) - \left(L \times (X(t) - GX_r(t)) + r_3 \times (X(t) - GX_r(t))\right) rand < 0.5 \end{cases} \tag{28}$$

where $X(t)$ and $GX(t + 1)$ denote the gorilla's current position vector and the potential of the gorilla's position vector in the subsequent t iterations, while $rand$, r_1, r_2, and r_3 denote random numbers between 0 and 1.

Before the optimization process, you will need to choose a value between 0 and 1 for the parameter known as *"p"*, which indicates the likelihood of selecting a migration plan that leads to an unidentified position. The X_r and GX_r each represents a single gorilla chosen from the entire population and one of the vectors of gorilla candidate positions that can be chosen randomly, respectively. The variables' lower limit (LL) and the upper limit (UL) are denoted by their corresponding initials. Eqs. (29), (31), and (32) can be used to provide a mathematical representation of the values of the variables C, L, and H, respectively.

$$C = F \times \left(1 - \frac{It}{MaxIt}\right) \tag{29}$$

$$F = \mathrm{Cos}\left(2 \times r_4\right) + 1 \tag{30}$$

$$L = C \times l \tag{31}$$

$$H = Z \times X\left(t\right) \tag{32}$$

$$Z = [-C, C] \tag{33}$$

The cosine function and random values from 0 to 1. l and Z represent random values between [-1, 1] and [-C, C]. At the end of the exploration phase, the cost of all GX solutions is reviewed, and if *GX*(t) *X*(*t*), *GX*(*t*) becomes the best solution (silverback).

5.2.2. Exploitation Phase

Following the silverback and rivalry for adult females are GTO exploitation methods. Using C in Eq. (29) and the specified parameter W, one of two tactics can be chosen, as shown next. The silverback gorilla leads his troop in making decisions and finding food. $C > W$ selects this strategy. The equation describes this behavior.

$$GX(t+1) = L \times M \times (X(t) - X_{Silverback}) + X(t) \tag{34}$$

The gorilla position vector is represented by *X*(*t*), whereas the silverback gorilla position vector, which provides the optimal answer, is represented by $X_{Silverback}$.

$$M = \left(\left|\frac{1}{N}\right) \sum_{i=1}^{N} GX_i(t)\right|)^g)^{\left(1/g\right)} \tag{35}$$

It should be illustrated where each potential Gorilla's vector is located in iteration t, where *N* is the number of Gorillas.

$$g = 2^L \tag{36}$$

L can be calculated using Eq. (31). If *C* is greater than *W*, the second strategy assigned for the exploitation phase is competition for adult females. When adolescent gorillas reach their full maturity, they compete fiercely with other males for the opportunity to mate with adult females. The mathematical representation of this behavior can be found in Eq. (37).

$$GX(i) = X_{Silverback} - (X_{Silverback} \times Q - X(t) \times (Q) \times A) \tag{37}$$

$$Q = 2 \times r_5 - 1 \tag{38}$$

$$A = \beta \times E \tag{39}$$

$$E = \begin{cases} N_1, rand \geq 0.5 \\ N_2, rand \leq 0.5 \end{cases} \tag{40}$$

While the symbol r_5 represents random values in the range [0, 1], the variable *Q* simulates the impact force, which may be the solution to Eq. (38). In the event of a fight, the coefficient A stands for a vector that shows the level of violence, and this vector's value can be calculated using the Eq. (39). In Eq. (39), the parameter has a value that was determined before the optimization procedure, and variable *E* is used to mimic violence's influence on the solutions' dimensions.

After the exploitation phase, a group formation operation is carried out. During this operation, the cost of every *GX* solution is calculated. If the cost of *GX*(*t*) is lower than the cost of *X*(*t*), the *GX*(*t*) solution is substituted for the *X*(*t*) solution, and the best solution that can be obtained from the entire population is referred to as a silverback.

6. RESULT DISCUSSION & CASE STUDY ANALYSIS

The proposed program is implemented on a personal computer with a 2.4 GHz Intel (R) Core (TM) i3 -7100 CPU. The computer also has 8 GB of RAM, which was used to replicate the study in a programming environment called MATLAB R2019a. MATLAB's artificial gorilla troop optimization techniques solve the optimization challenge. To prove the validity of the methodology, this study analyses 6 test cases.

6.1. Test Case 1. Existing Radial Distribution System

The units are put through their paces in this test scenario using the IEEE 33-Bus radial distribution system. The system has a voltage of 12.66kV, a load size of 3.715MW, and a voltage of 2.3MVar [51]. There are 33 buses and 32 lines in total.

According to the IEEE 33 RDS, the typical losses under full load conditions are 202.67 kW. In this system, the minimum voltage is 0.95p. u while the maximum is 1.05p.u. The magnitude profile of the system voltage is shown in Fig. 7. The lowest voltage was found on Bus 21, at 0.92 p.u. When comparing the voltage profile before and after the installation of SST with Wind and PV units, you can see a significant improvement in the latter.

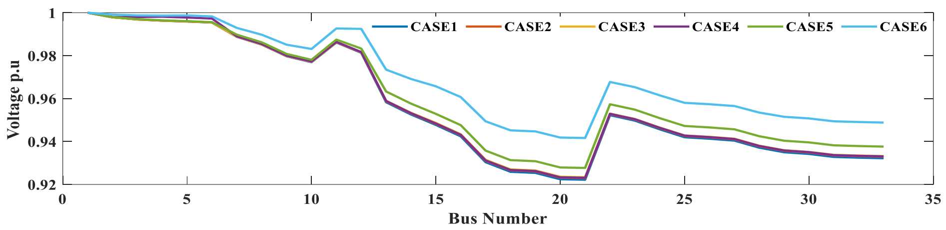

Fig. 7 Voltage magnitude profile of all six cases

6.2. Test Case 2. Analysis of SST Position with DT losses

Analysis position of SST at three positions with passive distribution network without any DG, BES. However, considering DT losses which have an impact on total losses. Fig. 8. shows the losses of the distribution transformer along with the total installed capacity. Optimal placement of SST at three locations without any DG considered in this case, as shown in Table 4.

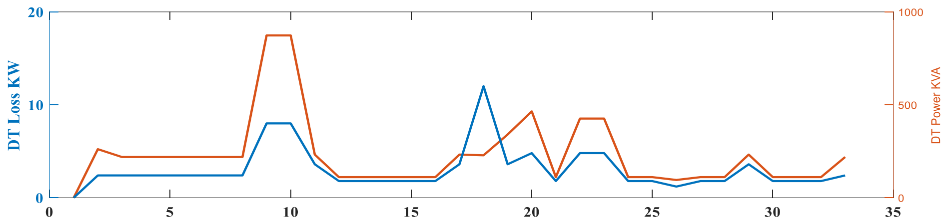

Fig. 8 DT losses along with installed capacity

6.3. Test Case 3. SST position with one DG (WT)

In this scenario, analyze the position of SST at one location with DG (WT). Overrating by 10% changes grid reactive power QSSTG. While running this case simulations, bus 21 with

500kVA capacity obtained the optimal placement of SST and Wind turbine, while assessing SST grid RPA. Hence, proving SST stage-I RPA in all circumstances. Table 4 shows the optimal placement of SST and wind turbine with their location, respectively, as discussed in the case.

6.4. Test Case 4. SST position with one DG (PV)

In this scenario, analyze the position of SST at one location with DG (PV). The grid reactive power QSSTG is varied by changing the percentage of overrating with an increment of 10%. While running this case, simulations of bus 21 with 500kVA capacity were obtained for the optimal placement of SST and PV. As shown in Table 4.

6.5. Test Case 5. SST position with one BES

In this scenario, analyze the position of SST at one location with BES. The grid reactive power QSSTG is varied by changing the percentage of overrating with an increment of 10%. While running this case, simulations bus 21 with 500kVA capacity obtained the optimal placement of SST and BES, as shown in Table 3. Fig. 9(a) shows that the active power consumption of the grid seldom shifts while examining the impact of grid RPA on the SST. So, the SST has reached the first step of its RPA capacity. Reactive power demand decreases as λ rises, as shown in Fig. 9(b).

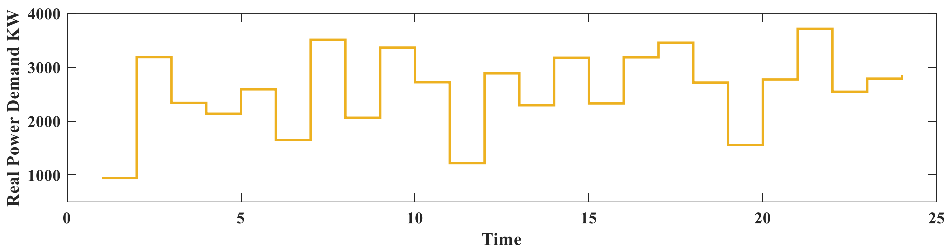

(a)

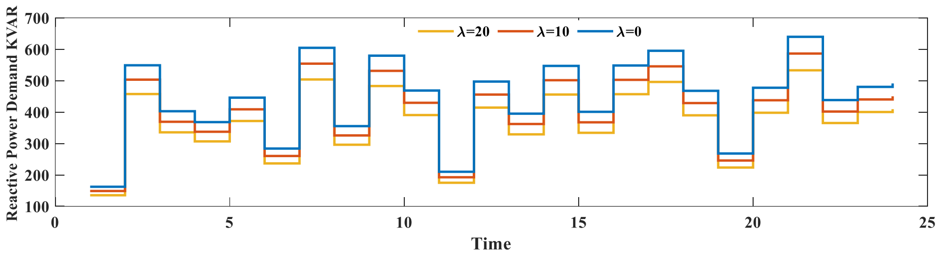

(b)

Fig. 9 (a) Real power demand (b) Reactive power demand

Table 3 Optimal solutions of case 6. (λ = 20) Using Gorilla Troop Optimization

SST Power kVA			SST Location			No. of W_T		W_T Location		No. of PV		PV Location		No. of BES		BES Location		*f1*	*f2*
127	**245**	**128**	**18**	**21**	**33**	**6**	**2**	**8**	**9**	**1**	**2**	**9**	**12**	**1**	**3**	**2**	**20**	***0.426***	***1183.7***
127	245	128	18	21	33	5	3	7	10	2	3	8	18	2	2	5	18	*0.412*	*1186.9*
127	245	128	18	21	33	7	1	11	9	1	2	9	20	3	1	6	21	*0.401*	*1250.6*
127	245	128	18	21	33	6	2	20	3	4	1	7	21	4	1	8	12	*0.351*	*1296.0*
127	245	128	18	21	33	4	4	6	15	6	2	8	20	1	3	2	20	*0.252*	*1300.2*
127	245	128	18	21	33	5	3	3	9	3	4	5	11	1	2	7	15	*0.238*	*1419.9*
127	245	128	18	21	33	6	2	8	9	1	2	9	12	5	1	6	12	*0.189*	*1679.2*
127	245	128	18	21	33	3	5	10	7	3	2	8	12	3	2	8	12	*0.077*	*2281.3*
127	245	128	18	21	33	7	1	3	15	5	2	6	18	1	3	2	20	*0.070*	*2368.5*

6.6. Test Case 6. SST position at three locations with Two DG (WT, PV) and BES

In this scenario, analyze the position of SST at three locations with (WT, PV) and BES. Fig 10 (a) illustrates the optimal solution of Gorilla Troop optimization for case 6, while the stage-I overrating is increased 10%.by the optimization obtained by overrating 20% is illustrated in Table 3. While running this case, simulations, bus 18, 21, 33 127,245, and 128 kVA capacity were obtained for the optimal placement of SST and DG in different locations, and the objective function value significantly improved. The analysis is compared with each λ value as shown in Fig. 10(b) and 10(c), and the comparison is illustrated in Table 5. Additionally, after the simulation of case 6, the reactive power demand is decreasing compared to other cases.

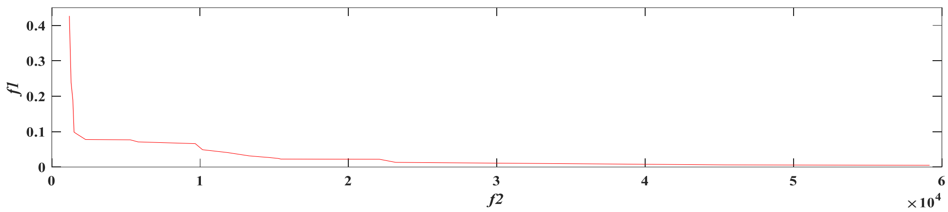

(a)

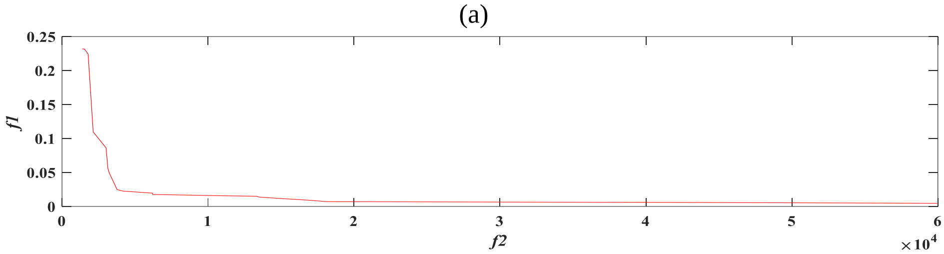

(b)

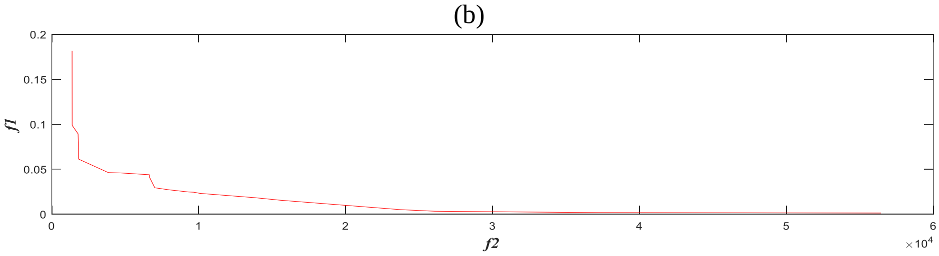

(c)

Fig. 10 (a) λ = 20 (b) λ = 10 (c) λ = 0

Table 4 Optimal Placement of SST, DG, and BES in different test cases

Test Case No.	SST Power kVA	SST Location	No. of W_T	W_T Location	No. of PV	PV Location	No. of BES	BES Location
2	127 245 128	18 21 33	-	-	-	-	-	-
3	500	21	9	26	-	-	-	-
4	500	21	-	-	3	27	-	-
5	500	21	-	-	-	-	9	19

Similarly, power losses are also decreasing, as shown in Figure 11 and Figure 12, respectively. Figure 13 illustrates the minimum voltage magnitude for each scenario, which can be used to check whether or not the Voltage improvement objective described in (20) has been met. The most considerable voltage improvement was found in Test Case 6, which supported both active and reactive power. It is also determined that 1.0 p.u. represents the greatest significant magnitude of voltage for each circumstance.Similarly, power losses are also decreasing, as shown in Fig. 11 and Fig. 12, respectively. Fig. 13 illustrates the minimum voltage magnitude for each scenario, which can be used to check whether or not the Voltage improvement objective described in Eq. (20) has been met. The most considerable voltage improvement was found in Test Case 6, which supported both active and reactive power. It is also determined that 1.0 p.u. represents the greatest significant magnitude of voltage for each circumstance. To validate the results of GTO the comparative analysis procedure is further carried on through the PSO and GA optimization techniques in the same way as adopted in Table 3 for the (λ=20) and Table 6 shows comparison results. The results confirm the effectiveness of the case study carried out in this work.

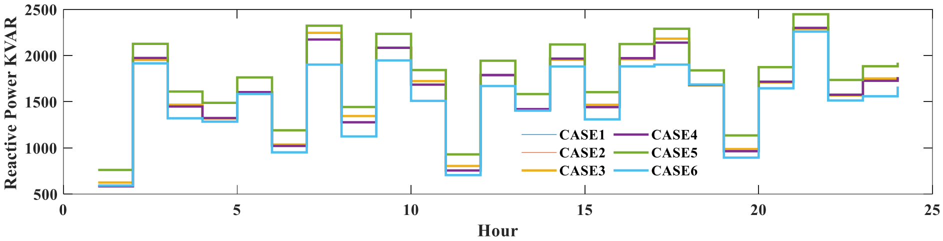

Fig. 11 Reactive power decrement after SST and DG placement of all the test cases

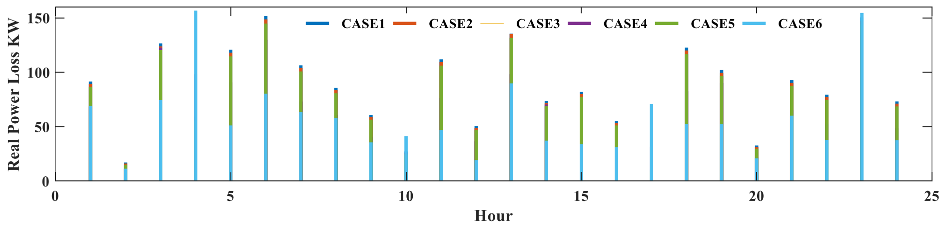

Fig. 12 Actual power loss for each test case

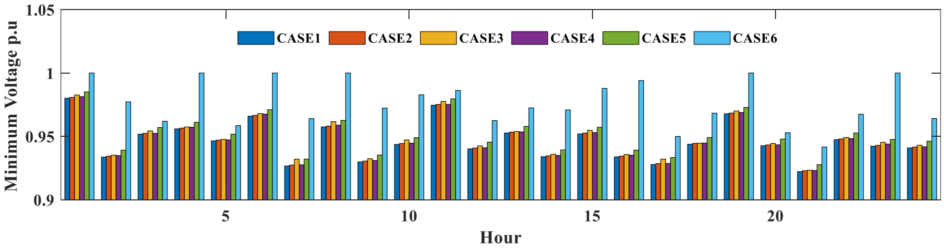

Fig. 13 The minimum voltage that can be applied is listed for each test case

Table 5 The optimal solution of case 6 for all the λ values

Method	λ(%)	SST Power	SST Location	No. W_T	W_T Location	No. PV	PV Location	No. BES	BES Location	F1	F2
GTO	20	127 245 128	18 21 33	6 2	8 9	1 2	9 12	1 3	2 20	0.426	1183.7
	10	127 245 128	18 21 33	6 2	8 9	1 2	9 12	1 3	2 20	0.245	1386.9
	0	127 245 128	18 21 33	6 2	8 9	1 2	9 12	1 3	2 20	0.184	1381.0

Table 6 The Comparison results of GTO, GA, and PSO

Method	λ(%)	SST Power	SST Location	No. W_T	W_T Location	No. PV	PV Location	No. BES	BES Location	F1	F2
GTO	20	127 245 128	18 21 33	6 2	8 9	1 2	9 12	1 3	2 20	0.426	1183.7
GA	20	127 245 128	18 21 33	6 2	8 9	1 2	9 12	1 3	2 20	0.397	1198.9
PSO	20	127 245 128	18 21 33	6 2	8 9	1 2	9 12	1 3	2 20	0.395	1205.8

7. Conclusion

The exploration of multiple Distributed Generators (DGs), which include wind turbines and solar panels, along with Battery Energy Storage (BES), is underway as promising options for providing dual reactive power support. These measures aim to reduce power losses and enhance voltage levels within radial distribution systems. The Gorilla Troop Optimization algorithm has been instrumental in determining the optimal quantity of Solid-State Transformers (SSTs), DG units, and BES installations. To make sense of the data, including load demand, solar irradiance, and wind speed, the K-medoid method is employed. Six simulated scenarios have been utilized to investigate the impact of integrating SSTs with

DG technologies such as Wind Turbines (WT), Photovoltaics (PV), and BES within a radial distribution system. The integration of DG units, either individually or in conjunction with appropriately sized SSTs, has led to reductions in power losses and improvements in voltage profiles. This study has successfully enhanced the voltage profile beyond the current configuration, achieving an 82.36% reduction in active power losses when optimized SSTs with dual reactive power support and variable DG are considered, in contrast to the existing distribution system. Additionally, reactive power losses have been decreased by 86.36%, and the voltage profile has significantly improved, rising from 0.92 p.u. to 1.0 p.u., indicating a higher value. Reactive power consumption has been reduced by 71.19%. Through the amalgamation of SSTs and DG systems, this research introduces a novel approach to addressing long-standing challenges associated with high distribution system losses and low voltage levels. Overcoming barriers such as high manufacturing costs, escalating losses, and equipment restrictions can be achieved. While transitioning from conventional Distribution Transformers (DTs) to SSTs requires a comparable timeframe, advancements in power electronics and semiconductors may help mitigate technological barriers. This technique has considerable promise for renewable energy integration, enhancements, and DNP areas, necessitating further research and analysis. Future research will be investigated by use of the following equipment to analyze the losses and voltage profile enhancement in the distribution network planning in a power distribution system with auxiliary functions provided by SST.

- Shunt Capacitors banks
- Unified Power Quality Conditioner (UPQC)
- A Distribution Static Synchronous Compensator (D-STATCOM).

REFERENCES

[1] A. Gantayet and D. K. Dheer,"A Data-Driven Approach to Support Voltage Profiles & Loss Reduction in Wind Generator Integrated Active Distribution Network Considering Solid-State Transformers with Twofold Reactive Power Compensation", *Energy Sources, Part A: Recovery, Utili. Environ. Eff.*, pp. 1-24, Dec. 2021.

[2] M. S. Shaikh, S. Raj, R. Babu, S. Kumar and K. Sagrolikar, "A Hybrid Moth–Flame Algorithm with Particle Swarm Optimization with Application in Power Transmission and Distribution", *Decis. Anal. J.*, vol. 6, p. 100182, March 2023.

[3] A. Gantayet and D. K. Dheer, "A Probabilistic Approach for Reactive Power Compensation in an Active Distribution Network with Wind Based Renewable Integration", In Proceedings of the IEEE International Conference on Emerging Frontiers in Electrical and Electronic Technologies (ICEFEET), 2020, pp. 1-6.

[4] M. S. Shaikh, S. Raj, M. Ikram and W. Khan, "Parameters Estimation of AC Transmission Line by an Improved Moth Flame Optimization Method", *J. Electr. Syst. Inf. Technol.*, vol. 9, p. 25, Dec. 2022.

[5] M. H. Hassan, S. Kamel, M. S. Shaikh, T. Alquthami and A.G. Hussien, "Supply-Demand Optimizer for Economic Emission Dispatch Incorporating Price Penalty Factor and Variable Load Demand Levels", *IET Gener. Transm. Distrib.*, vol. 17, pp. 3211-3231, June 2023.

[6] M. S. Alam, F. S. Al-Ismail, A. Salem and M. A. Abido, "High-level Penetration of Renewable Energy Sources Into Grid Utility: Challenges and Solutions", *IEEE Access*, vol. 8, pp. 190277-190299, Oct. 2020.

[7] D. Stanelyte and V. Radziukynas, "Review of Voltage and Reactive Power Control Algorithms in Electrical Distribution Networks", *Energies*, vol. 13, p. 58, Dec. 2019.

[8] M. S. Shaikh, C. Hua, M. Hassan, S. Raj, M. A. Jatoi and M. M. Ansari, "Optimal Parameter Estimation of Overhead Transmission Line Considering Different Bundle Conductors with the Uncertainty of Load Modeling", *Optim. Control Appl. Methods*, vol. 43, pp. 652-666, Aug. 2021.

[9] S. Kumar, C. K. Faizan Ur Rehman, S. A. Shaikh and A. A Sahito, "Voltage Improvement and Power Loss Reduction Through Capacitors in Utility Network", In Proceedings of the IEEE International

Conference on Computing, Mathematics and Engineering Technologies: Invent, Innovate and Integrate for Socioeconomic Development (iCoMET), 2018, pp. 1-5.

[10] M. Jiang, Q. Guo, H. Sun and H. Ge, "Leverage Reactive Power Ancillary Service Under High Penetration of Renewable Energies: An Incentive-Compatible Obligation-Based Market Mechanism", *IEEE Trans. Power Syst.*, vol. 37, pp. 2919-2933, Nov. 2021.

[11] S. Rajamand, "Loss Cost Reduction and Power Quality Improvement with Applying Robust Optimization Algorithm for Optimum Energy Storage System Placement and Capacitor Bank Allocation", *Int. J. Energy Res.*, vol. 44, pp. 11973-11984, Sept. 2020.

[12] I. Molver and S. Chowdhury, "Alternative Approaches for Analysing the Impact of Distributed Generation on Shunt Compensated Radial Medium Voltage Networks", *Comput. Electr. Eng.*, vol. 85, pp. 106676, July 2020.

[13] X. Liang and C. Andalib-Bin-Karim, "Harmonics and Mitigation Techniques Through Advanced Control in Grid-Connected Renewable Energy Sources: A Review", *IEEE Trans. Ind. Appl.*, vol. 54, pp. 3100-3111, April 2018.

[14] A. H. Elmetwaly, A. A. Eldesouky and A. A. Sallam, "An Adaptive D-FACTS for Power Quality Enhancement in an Isolated Microgrid", *IEEE Access*, vol. 8, pp. 57923-57942, March 2020.

[15] F. H. Gandoman, A. Ahmadi, A. M. Sharaf, P. Siano, J. Pou, B. Hredzak and V. G. Agelidis, "Review of FACTS Technologies and Applications for Power Quality in Smart Grids with Renewable Energy Systems", *Renew. Sustain. Energy Rev.*, vol. 82, pp. 502-514, Feb. 2018.

[16] A. A. Abdelsalam and A. M. Sharaf, "A Novel Facts Compensation Scheme for Power Quality Improvement in Wind Smart Grid", In Proceedings of the 25th IEEE Canadian Conference on Electrical and Computer Engineering: Vision for a Greener Future (CCECE), 2012, pp. 1-4.

[17] P. Jyotishi and P. Deeparamchandani, "Mitigate Voltage Sag/Swell Condition and Power Quality Improvement in Distribution Line Using D-STATCOM", *J. Eng. Res. Appl.*, vol. 3, pp. 667-674, 2013.

[18] V. Chaudhary, A. Bhargava and S. Verma, "Power Quality Enhancement Using Unified Power Flow Controller in Grid Connected Hybrid PV/Wind System", In Proceedings of the IEEE 4th International Conference on Communication and Electronics Systems (ICCES), 2019, pp. 2064-2069.

[19] E. Jamil, S. Hameed, B. Jamil and Qurratulain, "Power Quality Improvement of Distribution System with Photovoltaic and Permanent Magnet Synchronous Generator Based Renewable Energy Farm Using Static Synchronous Compensator", *Sustain. Energy Technol. Assessments*, vol. 35, pp. 98-116, Oct. 2019.

[20] B. Ismail, N. I. Abdul Wahab, M. L. Othman, M. Radzi, K. N. Vijyakumar and M. N. Mat Naain, "A Comprehensive Review on Optimal Location and Sizing of Reactive Power Compensation Using Hybrid-Based Approaches for Power Loss Reduction, Voltage Stability Improvement, Voltage Profile Enhancement and Loadability Enhancement", *IEEE Access*, vol. 8, pp. 222733-222765, Dec. 2020.

[21] O. D. Montoya and W. Gil-González, "Dynamic Active and Reactive Power Compensation in Distribution Networks with Batteries: A Day-Ahead Economic Dispatch Approach", *Comput. Electr. Eng.*, vol. 85, p. 106710, July 2020.

[22] M. Azeroual, T. Lamhamdi, H. El. Moussaoui and H. El. Markhi, "Intelligent Energy Management System of a Smart Microgrid Using Multiagent Systems", *Arch. Electr. Eng.*, vol. 69, pp. 23-38, 2020.

[23] K. M. Rafi and P. V. N. Prasad, "Comparison of Control Algorithms for Power Factor Correction in a Distribution System Using DSTATCOM", In Proceedings of the IEEE International Conference on Power, Control, Signals and Instrumentation Engineering (ICPCSI), 2017, pp. 1736-1741.

[24] H. Lotfi, M. Samadi and A. Dadpour, "Optimal Capacitor Placement and Sizing in Radial Distribution System Using an Improved Particle Swarm Optimization Algorithm", In Proceedings of the IEEE 21st Electrical Power Distribution Network Conference (EPDC) 2016, pp. 147-152.

[25] A. S. Hassan, Y. Sun and Z. Wang, "Multi-Objective for Optimal Placement and Sizing DG Units in Reducing Loss of Power and Enhancing Voltage Profile Using BPSO-SLFA", *Energy Reports*, vol. 6, pp. 1581-1589, Nov. 2020.

[26] T. T. Nguyen, B. H. Dinh, T. D. Pham and T. T. Nguyen, "Active Power Loss Reduction for Radial Distribution Systems by Placing Capacitors and PV Systems with Geography Location Constraints", *Sustainability*, vol. 12, p. 7806, September 2020.

[27] A. N. Hussain, W. K. Shakir Al-Jubori and H. F. Kadom, "Hybrid Design of Optimal Capacitor Placement and Reconfiguration for Performance Improvement in a Radial Distribution System", *J. Eng.*, vol. 2019, p,1696347, Dec. 2019.

[28] O. Eo, A. To, O. Ik and A. I. Oo, "Optimal sitting and sizing of shunt capacitor for real power loss reduction on radial distribution system using firefly algorithm: A case study of Nigerian system", *Energy Sources, Part A: Recovery, Util. Environ. Eff.*, vol. 45, pp. 5776-5788, Oct. 2019.

[29] M. S. Shaikh, C. Hua, S. Raj, S. Kumar, M. Hassan, M. M. Ansari and M. A. Jatoi, "Optimal Parameter Estimation of 1-phase and 3-phase Transmission Line for Various Bundle Conductor's Using Modified Whale Optimization Algorithm", *Int. J. Electr. Power Energy Syst.*, vol. 138, p. 107893, June 2022.

[30] M. S. Shaikh, C. Hua, M. A. Jatoi, M. M. Ansari and A. A. Qader, "Application of Grey Wolf Optimisation Algorithm in Parameter Calculation of Overhead Transmission Line System", *IET Sci. Meas. Technol.*, vol. 15, pp. 218-231, Feb. 2021.

[31] S. G. Shekarappa, S. Mahapatra and S. Raj, "Voltage Constrained Reactive Power Planning Problem for Reactive Loading Variation Using Hybrid Harris Hawk Particle Swarm Optimizer", *Electr. Power Compon. Syst.*, vol. 49, pp. 421-435, Sept. 2021.

[32] C. K. Shiva, S. S. Gudadappanavar, B. Vedik, R. Babu, S. Raj and B. Bhattacharyya, "Fuzzy-Based Shunt VAR Source Placement and Sizing by Oppositional Crow Search Algorithm", *J. Control Autom. Electr. Syst.*, vol. 33, pp. 1576-1591, Feb. 2022.

[33] M. S. Shaikh, C. Hua, M. A. Jatoi, M. M. Ansari and A. A. Qader, "Parameter Estimation of AC Transmission Line Considering Different Bundle Conductors Using Flux Linkage Technique", *IEEE Can. J. Electr. Comput. Eng.*, vol. 44, pp. 313-320, June 2021.

[34] I. Syed, V. Khadkikar and H. H. Zeineldin, "Loss Reduction in Radial Distribution Networks Using a Solid-State Transformer", *IEEE Trans. Ind. Appl.*, vol. 54, pp. 5474-5482, May 2018.

[35] D. K. Mishra, M. J. Ghadi, L. Li, M. J. Hossain, J. Zhang, P. K.Ray and A. Mohanty, "A Review on Solid-State Transformer: A Breakthrough Technology for Future Smart Distribution Grids", *Int. J. Electr. Power Energy Syst.*, vol. 133, p. 107255, Dec. 2021.

[36] D. Shah and M. L. Crow, "Online Volt-Var Control for Distribution Systems with Solid-State Transformers", *IEEE Trans. Power Deliv.*, vol. 31, pp. 343-350, July 2015.

[37] X. Gao, F. Sossan, K. Christakou, M. Paolone and M. Liserre, "Concurrent Voltage Control and Dispatch of Active Distribution Networks by Means of Smart Transformer and Storage", *IEEE Trans. Ind. Electron.*, vol. 65, pp. 6657-6666, Nov. 2017.

[38] M. T. A. Khan, A. A. Milani, A. Chakrabortty and I. Husain, "Dynamic Modeling and Feasibility Analysis of a Solid-State Transformer-Based Power Distribution System", *IEEE Trans. Ind. Appl.*, vol. 54, pp. 551-562, Sept. 2017.

[39] G. Guerra and J. A. Martinez-Velasco, "A Solid State Transformer Model for Power Flow Calculations", *Int. J. Electr. Power Energy Syst.*, vol. 89, pp. 40-51, July 2017.

[40] I. Syed, V. Khadkikar and H. H. Zeineldin, "Loss Reduction in Radial Distribution Networks Using a Solid-State Transformer", *IEEE Trans. Ind. Appl.*, vol. 54, pp. 5474-5482, May 2018.

[41] D. E. Goldberg and J. H. Holland, "Genetic Algorithms and Machine Learning", *Machine Learning,* vol. 3, pp. 95-99, 1988.

[42] J. Kennedy and R. Eberhart, "Particle swarm optimization", In Proceedings of the IEEE ICNN'95-International Conference on Neural Networks, 1995, pp. 1942-1948.

[43] A. Clifton, B. M. Hodge, C. Draxl, J. Badger and A. Habte, "Wind and Solar Resource Data Sets", *Wiley Interdiscip. Rev. Energy Environ.*, vol. 7, p. e276, Dec. 2017.

[44] S. Barik and D. Das, "Determining the Sizes of Renewable DGs Considering Seasonal Variation of Generation and Load and Their Impact on System Load Growth", *IET Renewable Power Generation*, vol. 12, pp. 1101-1110, June 2018.

[45] K. M. Kalantari and A. Askarzadeh, "Optimal MV/LV Transformer Allocation in Distribution Network for Power Losses Reduction and Cost Minimization: A New Multi-Objective Framework", *Int. Trans. Electr. Energy Syst.*, vol. 30, p. e12361, Feb. 2020.

[46] J. E. Huber and J. W. Kolar, "Volume/Weight/Cost Comparison of a 1MVA 10 kV/400 V Solid-State Against a Conventional Low-Frequency Distribution Transformer", In Proceedings of the IEEE Energy Conversion Congress and Exposition (ECCE), 2014, pp. 4545-4552.

[47] J. H. Teng, "A Direct Approach for Distribution System Load Flow Solutions", *IEEE Trans. Power Delivery*, vol. 18, pp. 882-887, July 2003.

[48] H. S. Park and C. H. Jun, "A Simple and Fast Algorithm for K-Medoids Clustering", *Expert Syst. Appl.*, vol. 36, pp. 3336-3341, March 2009.

[49] M. S. Shaikh, S. Raj, S. Abdul Latif, W. F. Mbasso and S. Kamel, "Optimizing Transmission Line Parameter Estimation with Hybrid Evolutionary Techniques", *IET Gener. Transm. Distrib.*, vol. 18, pp. 1795-814, April 2024.

[50] B. Abdollahzadeh, G. F. Soleimanian and S. Mirjalili, "Artificial Gorilla Troops Optimizer: A New Nature-Inspired Metaheuristic Algorithm for Global Optimization Problems", *Int. J. Intell. Syst.*, vol. 36, pp. 5887-5958, July 2021.

[51] K. R. Guerriche and T. Bouktir, "Maximum Loading Point in Distribution System with Renewable Resources Penetration", In Proceedings of the IEEE International Renewable and Sustainable Energy Conference (IRSEC), 2014, pp. 481-486.